seems to be in contradiction with the qualitative prediction of Herzberg-Teller theory[25] where mode 6b having b_2 symmetry should appear in $^3B_2$-$^3B_2$ as well as in $^3A_1$-$^3B_2$ transitions, as mentioned in the introduction. In order to account for that, explicit calculation[44] of vibronic coupling matrix elements should be made. Given the relative oscillator strengths of the first two electronic transitions (see Table I) and the presence of mode 6b in the more intense emission (i.e., $^3A_1$-$^3B_2$), this borrowing mechanism should involve higher $^3A_1$ excited states having large oscillator strengths f, as, for example, level T_5 whose f is larger than 0.1 in most cases (see Table I).

Conclusion

Information obtained from vibronic structures of fluorescence spectra and from quantum chemical calculations reveals some parentage between *m*-xylylene biradicals and benzyl-type monoradicals. In both cases, the two first electronic transitions, involving doublet D states for monoradicals and triplet T states for biradicals, are close in energy and have very low oscillator strengths. However theory predicts three or four singlet states between the ground and the lowest excited triplet state in biradicals (see Figure 3b), whereas no excited electronic level is found below the fluorescence state in benzyl-type radicals, the first quadruplet state being at least 1 eV above the first excited doublet.[36] The presence of singlet levels below the emitting triplet introduces in biradicals new relaxation paths for radiationless transitions to the ground state T_0, such as $T_1 \rightarrow S_n$ (n = 1-3, 4) and $S_0 \rightarrow T_0$ intersystem crossings together with $T_1 \rightarrow T_0$ and $S_n \rightarrow S_0$ internal conversions. In monoradicals, the $D_1 \rightarrow D_0$ internal conversion is the only process to compete with the $D_1 \rightarrow D_0$ fluorescence.

Let us now discuss the theoretically determined ordering of the two close-lying excited $^3B_2$ and $^3A_1$ states. For *m*-xylylene, this ordering depends on the approximations used in the calculations. For example, the symmetry of the lowest excited triplet T_1 changes from A_1 to B_2 when the number of configurations used in the CI increases from 54 to 172. The question then arises, what is the meaning of the ordering predicted for the two close-lying excited $^3B_2$ and $^3A_1$ states of *m*-xylylene biradicals and its dependence with methyl substitution as depicted in Table I? Moreover, the empirical additivity rule found on the observed transition energies for the whole series of methylated *m*-xylylene biradicals could be interpreted as an indication that the lowest excited triplet is of the same symmetry in all the molecules tested. To clarify the situation, we intend to determine the symmetry of the fluorescent state of *m*-xylylene biradicals by means of the multistep photoselection technique.[45]

Acknowledgment. We are grateful to Dr. Siebrand who, as a referee, suggested to us the empirical additivity rule.

Registry No. 1,2,3-Trimethylbenzene biradical, 100859-21-0; prehnitene biradical, 100859-22-1; hexamethylbenzene biradical, 100859-23-2.

(44) Orlandi, G. *Chem. Phys. Lett.* **1976**, *44*, 277.

(45) Johnson, P. M.; Albrecht, A. C. *J. Chem. Phys.* **1968**, *48*, 851.

Formation of Ionic Transition Metal Carbonyl Cluster Fragments by Ion-Molecule Reactions. 2. The $Co(CO)_3(NO)$ and $Ni(CO)_4$ Systems

DonnaJean Anderson Fredeen and David H. Russell*

Contribution from the Department of Chemistry, Texas A&M University, College Station, Texas 77843. *Received September 10, 1985*

Abstract: The ion-molecule reaction chemistry of $Co(CO)_3(NO)$ and $Ni(CO)_4$ is presented. Ionic cluster fragments of the type $M_x(CO)_y(NO)_z^+$ are formed from the reaction of the fragment ion $M(CO)_a(NO)_b^+$ with its respective neutral. The relative reaction rate and electron deficiency of the ionic cluster fragments are used to estimate the bond order of the ionic cluster fragments. Comparison of the $Cr(CO)_6$, $Fe(CO)_5$, $Co(CO)_3(NO)$, and $Ni(CO)_4$ systems shows that the ionic cluster fragments can be divided into two catagories: (1) ionic cluster fragments with simple polyhedral structures and (2) ionic cluster fragments which exhibit unusual binding of the ligands and/or metals, resulting in ionic cluster fragments with high bond orders. These two classes of ionic cluster fragments are discussed in terms of the interrelationship of the reactivity/electron deficiency model and the cluster valence molecular orbital model developed by Lauher.

In a recent paper,[1] we reported on the formation of ionic cluster fragments of $Cr_x(CO)_y^+$ and $Fe_x(CO)_y^+$ by gas-phase ion-molecule reactions. In this report, we wish to extend this work to include ionic cluster fragments of $Ni_x(CO)_y^+$ and $Co_x(CO)_y(NO)_z^+$. Although the ion-molecule chemistry of these various transition-metal carbonyl systems are quite similar, there are substantial differences in the degree of coordination saturation/unsaturation for many of the ionic cluster fragments formed.

In our previous paper, we attempted to review the most pertinent literature on the gas-phase ion-molecule chemistry of ionic cluster fragments of transition metals as well as bare metal ions. Although such a review will not be duplicated here, we would like to reemphasize the earlier work by Ridge.[2] On the basis of studies of anionic cluster fragments of $Fe(CO)_5$, Ridge postulated a direct relationship between the electron deficiency and reactivity for ionic cluster fragments. That is, the reactivity increases as the electron deficiency (degree of coordination unsaturation) of an ionic cluster fragment increases. On the basis of this concept, Ridge suggested that the $Fe_2(CO)_x^-$ (x = 5-7) ionic cluster fragments contain a double metal-metal bond.

In our first paper,[1] Ridge's data analysis method was applied to the $Cr_x(CO)_y^+$ and $Fe_x(CO)_y^+$ cluster fragments. For example, the reaction of $Fe(CO)^+$ with neutral $Fe(CO)_5$ gives rise to product ions having reactivities that follow the predicted electron deficiencies assuming simple polyhedral structures. Conversely, the reaction of Fe^+ with $Fe(CO)_5$ gives rise to product ions having sharp discontinuities between reactivity and electron deficiencies.

(1) Fredeen, DonnaJean Anderson; Russell, David H. *J. Am. Chem. Soc.* **1985**, *107*, 3762.

(2) Wronka, J.; Ridge, D. P. *J. Am. Chem. Soc.* **1984**, *106*, 67.

0002-7863/86/1508-1860$01.50/0

However, if multiple metal-metal bonds and/or four-electron donor carbonyl ligands are considered, good agreement is obtained for reactivity vs. electron deficiency. That is, the low reactivity of some ionic cluster fragments can be attributed to changes in the metal-metal and metal-ligand bonding.

To extend these ideas further and to test the general relationship between reactivity and electron deficiency, we have studied the ion-molecule chemistry of $Co(CO)_3(NO)$ and $Ni(CO)_4$. The general ion-molecule reaction sequences for cluster formation for the $Co(CO)_3(NO)$ and $Ni(CO)_4$ systems are presented. The ionic cluster fragments formed in these two systems are then discussed in terms of the relative reactivities and degree of coordination saturation/unsaturation. In the last section of the paper comparisons are made for the $Cr(CO)_6$, $Fe(CO)_5$, $Co(CO)_3(NO)$, and $Ni(CO)_4$ systems. A detailed analysis of the ionic cluster fragments formed in the $Cr(CO)_6$, $Fe(CO)_5$, $Co(CO)_3(NO)$, and $Ni(CO)_4$ systems shows that two classes of product ions are formed: (1) ionic cluster fragments with simple polyhedral structures and (2) ionic cluster fragments which exhibit unusual binding of the ligands and/or metal, resulting in ionic cluster fragments with high bond orders. These two classes of ionic cluster fragments are discussed in terms of the interrelationship between the reactivity/electron deficiency model and the cluster valence molecular orbital model developed by Lauher.[3] A better understanding of the structure and bond order of these ionic cluster fragments facilitates the development of gas-phase systems which mimic catalytic reactions.

Experimental Section

All experiments were carried out with use of a standard Nicolet FTMS-1000 equipped with a 3T magnet and a cubic (2.5 cm × 2.5 cm × 2.5 cm) ion cell. Samples were introduced to the system with use of variable leak valves maintained at ambient temperatures. Typically, a sample pressure of ca. 1×10^{-7} torr, measured with a Granville-Phillips Gauge Controller Series 280, was employed for all studies. Electron impact ionization of the sample was performed with use of 50 eV (nominal) ionizing energy and 100 +/- 10 nanoamperes of emission current. The ion cell trapping voltage was typically maintained at 1.25 V (16.5 V/m).

Ion ejection techniques were used to mass-select a particular reactant ion. The procedures utilized for these studies have been described previously and are analogous to those used for collision-induced dissociation.[4] In all experiments, the ion ejection frequencies were selected so as to minimize the translational excitation of the reactant ion.[1]

A diagram depicting the experimental sequence is shown in Figure 1. The quench pulse removes any ions present in the cell before formation of new ions. The ionizing electron beam is pulsed on for approximately 5 ms. Once the sample is ionized, the ion ejection oscillators are swept over the desired mass range. A variable delay time between ion ejection and ion detection is used to control the ion-molecule reaction time.

Relative ion-molecule reaction rates and electron deficiencies were calculated as described previously.[1]

Results

In this section, the ion-molecule reactions of the $Co(CO)_3(NO)$ and $Ni(CO)_4$ systems are discussed. Electron impact ionization (50 eV nominal ionizing energy) of the $Co(CO)_3(NO)$ or $Ni(CO)_4$ produces a series of metal-containing ions, viz., $M(CO)_m(NO)_n^+$ (m = 0–x; n = 0–y). In order to study the ion-molecule chemistry of a specific ion, the reactant ion is mass-selected with ion ejection techniques.[5] Following the mass-selection step a suitable delay time is imposed during which time the ion undergoes reactions with the neutral molecule.[5]

The major advantage in using ion ejection techniques to select the primary reactant ion is to obtain relative reactivity data for the various reactant ions, i.e., M^+ or $M(CO)_y(NO)_z^+$, and to follow a specific sequence of reactions leading to cluster formation. In this study we have not attempted to measure absolute reaction rates. The instrument used for these studies is not equipped with devices for accurately measuring the pressure of the neutral. In the following sections, a detailed analysis for the cluster sequence of the $Co(CO)_3(NO)$ and $Ni(CO)_4$ systems is presented. Although the general reaction sequences for these systems have many similarities, each system manifests characteristic differences.

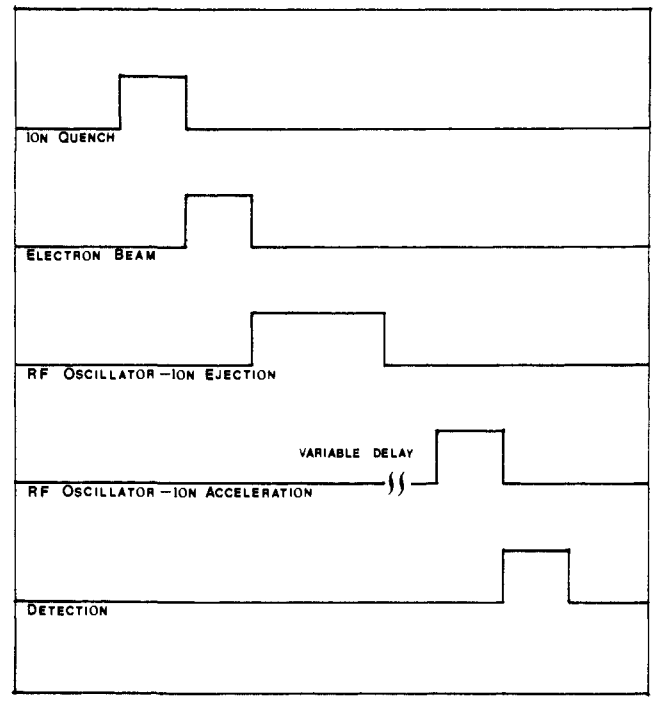

Figure 1. Diagram of the experimental sequence for FTMS.

$Co(CO)_3(NO)$. Direct ionization of $Co(CO)_3(NO)$ produces abundant ions corresponding to $Co(CO)_x(NO)_y^+$ (x = 0–2; y = 0–1). In this system there are pairs of ions, e.g., $Co(CO)^+$ and $Co(NO)^+$, that cannot be mass-selected with ion ejection methods without affecting the ion's translational energy.[1,6] Therefore, the chemistry of $Co(CO)^+$ and $Co(NO)^+$ was investigated simultaneously. For example, following ion ejection, both $Co(CO)^+$ and $Co(NO)^+$ remain to the cell and are allowed to react with the neutral. The product ions formed by reaction of $Co(NO)^+$ are of low abundance (<20% relative intensity); therefore, the reaction sequence was not studied in great detail. The most reactive ions in the $Co(CO)_3(NO)$ system are Co^+, $Co(CO)^+$, $Co(CO)_2^+$, and $Co(CO)_2(NO)^+$. It is the chemistry of these ions that we will emphasize in the following section.

The largest cluster fragment produced by reaction of Co^+ with $Co(CO)_3(NO)$ is $Co_6(CO)_6(NO)_5^+$. Although cluster fragments corresponding to $Co_7(CO)_7(NO)_5^+$ and $Co_8(CO)_8(NO)_6^+$ are formed at long reaction times (>1 s), the relative abundance of these ions is low (<20%) and we have not investigated these ions thoroughly. The $Co_6(CO)_6(NO)_5^+$ ion is formed by sequential reactions involving $Co_2(CO)_x(NO)^+$ (x = 1, 2), $Co_3(CO)_2(NO)_y^+$ (y = 1, 2), $Co_4(CO)_x(NO)_3^+$ (x = 2, 3), and $Co_5(CO)_x(NO)_4^+$ (x = 3, 4). A general reaction sequence is summarized in Scheme I. (Only the major (>20%) ionic cluster fragments are included

Scheme I

$$Co^+ + Co(CO)_3(NO) \rightarrow Co_2(CO)_x(NO)^+ \quad (x = 1, 2) \qquad (1)$$

$$Co_2(CO)_x(NO)^+ + Co(CO)_3(NO) \rightarrow Co_3(CO)_2(NO)_2^+ \qquad (2)$$

$$Co_3(CO)_2(NO)_2^+ + Co(CO)_3(NO) \rightarrow Co_4(CO)_{x+2}(NO)_3^+ \qquad (3)$$

$$Co_4(CO)_{x+2}(NO)_3^+ + Co(CO)_3(NO) \rightarrow Co_5(CO)_{x+3}(NO)_4^+ \qquad (4)$$

$$Co_5(CO)_{x+3}(NO)_4^+ + Co(CO)_3(NO) \rightarrow Co_6(CO)_{x+4}(NO)_5^+ \qquad (5)$$

(3) Lauher, Joseph W. *J. Am. Chem. Soc.* **1978**, *100*, 5305.

(4) For a discussion of ion cyclotron resonance spectrometry, double resonance, and ion-ejection techniques see: (a) Lehman, T. A.; Bursey, M. N. "Ion Cyclotron Resonance Spectrometry"; Wiley-Interscience: New York, 1976. (b) Gross, M. L.; Rempel, D. L. *Science* **1984**, *226*, 261. (c) Johlman, C. L.; White, R. L.; Wilkins, C. L. *Mass Spectrom. Rev.* **1983**, *2*, 389.

(5) (a) Armstrong, J. T.; Beauchamp, J. L. *Rev. Sci. Instrum.* **1969**, *40*, 123. (b) Cody, R. B.; Burnier, R. C.; Freiser, B. S. *Anal. Chem.* **1982**, *54*, 2225.

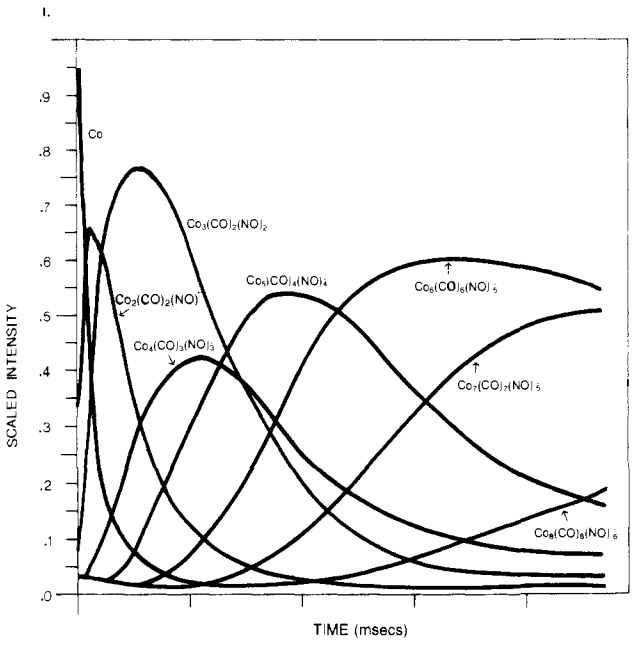

Figure 2. Temporal distribution of cluster fragments formed when Co^+ reacts with $Co(CO)_3(NO)$.

in the reaction scheme.) The general reaction scheme was confirmed by using ion ejection techniques and by following the temporal distribution of the product ions. A temporal distribution of the various ionic cluster fragments initiated by the Co^+ ion is shown in Figure 2. The data in Figure 2 give the relative abundance for each of the ionic cluster fragments, e.g., percent total ion current vs. time.

The clustering sequence for the $Co(CO)^+$ ion is very similar to that of the Co^+ ion. For example, $Co(CO)^+$ reacts with $Co(CO)_3(NO)$ to produce the dinuclear species $Co_2(CO)_x(NO)^+$ (x = 2-4) (reaction 6). An intense ion at m/z 262, corresponding to $Co_2(CO)_2(NO)_2^+$, is produced by $Co(NO)^+$ reacting with the neutral (reaction 7). However, the reactivity of the $Co_2(CO)_2(NO)_2^+$ ion is quite low and it does not give rise to any major trinuclear cluster fragments containing three nitrosyls. The $Co_2(CO)_x(NO)^+$ ionic cluster fragments react with $Co(CO)_3(NO)$ to produce $Co_3(CO)_2(NO)_2^+$ (reaction 8). This trinuclear species is very reactive and produces $Co_4(CO)_{x+1}(NO)_3^+$ (x = 2, 3) (reaction 9). This scheme (Scheme II) terminates with the formation of $Co_5(CO)_4(NO)_4^+$ from $Co_4(CO)_{x+1}(NO)_3^+$ reacting with the neutral (reaction 10).

Scheme II

$$Co(CO)^+ + Co(CO)_3(NO) \rightarrow Co_2(CO)_x(NO)^+ \quad (x = 2\text{-}4) \quad (6)$$

$$Co(NO)_+ + Co(CO)_3(NO) \rightarrow Co_2(CO)_3(NO)_2^+ \quad (7)$$

$$Co_2(CO)_x(NO)^+ + Co(CO)_3(NO) \rightarrow Co_3(CO)_2(NO)_2^+ \quad (8)$$

$$Co_3(CO)_2(NO)_2^+ + Co(CO)_3(NO) \rightarrow Co_4(CO)_{x+1}(NO)_3^+ \quad (9)$$

$$Co_4(CO)_{x+1}(NO)_3^+ + Co(CO)_3(NO) \rightarrow Co_5(CO)_4(NO)_4^+ \quad (10)$$

The reaction sequences for $Co(CO)_2^+$ and $Co(CO)_2(NO)^+$ are summarized in Schemes III and IV. The reaction sequence for $Co(CO)_2^+$ differs from that for Co^+ and $Co(CO)^+$ ion in that there is not a sequential addition of the NO ligand. For example, the clustering sequence for Co^+ contains the ions $Co_2(CO)_x(NO)^+$, $Co_3(CO)_2(NO)_2^+$, $Co_4(CO)_{x+2}(NO)_3^+$, $Co_5(CO)_{x+3}(NO)_4^+$, and $Co_6(CO)_{x+4}(NO)_5^+$. As each ionic cluster fragment adds a metal, it also adds a CO and NO ligand. However, in the clustering sequence for $Co(CO)_2^+$, the addition of a metal does not necessarily result in addition of a NO ligand. For example, reaction of the trinuclear cluster fragment $Co_3(CO)_4(NO)_2^+$ with neutral $Co(CO)_3(NO)$ gives rise to $Co_4(CO)_x(NO)^+$ (x = 4, 5). Further reaction of $Co_4(CO)_{x+1}(NO)^+$ produces $Co_5(CO)_4(NO)^+$ (reaction 15). As in the reactions of $Co(CO)^+$ (Scheme II), the reaction scheme for $Co(CO)_2^+$ (Scheme III) contains dinuclear fragments having two NO ligands. This results from $Co(CO)(NO)^+$ reacting with $Co(CO)_3(NO)$ (reaction 12). Once again, however, the $Co_2(CO)_x(NO)_2^+$ (x = 2, 3) ions are unreactive and do not produce any major trinuclear cluster fragments containing three nitrosyls.

Scheme III

$$Co(CO)_2^+ + Co(CO)_3(NO) \rightarrow Co_2(CO)_x(NO)^+ \quad (x = 3, 4) \quad (11)$$

$$Co(CO)(NO)^+ + Co(CO)_3(NO) \rightarrow Co_2(CO)_y(NO)_2^+ \quad (y = 2, 3) \quad (12)$$

$$Co_2(CO)_x(NO)^+ + Co(CO)_3(NO) \rightarrow Co_3(CO)_4(NO)_2^+ \quad (13)$$

$$Co_3(CO)_4(NO)_2^+ + Co(CO)_3(NO) \rightarrow Co_4(CO)_{x+1}(NO)^+ \quad (14)$$

$$Co_4(CO)_{x+1}(NO)^+ + Co(CO)_3(NO) \rightarrow Co_5(CO)_4(NO)^+ \quad (15)$$

Scheme IV

$$Co(CO)_2(NO)^+ + Co(CO)_3(NO) \rightarrow Co_2(CO)_x(NO)_2^+ \quad (x = 3, 4) \quad (16)$$

$$Co_2(CO)_x(NO)^+ + Co(CO)_3(NO) \rightarrow Co_3(CO)_{x+1}(NO)_y^+ \quad (y = 2, 3) \quad (17)$$

$$Co_3(CO)_{x+1}(NO)_y^+ + Co(CO)_3(NO) \rightarrow Co_4(CO)_4(NO)_3^+ \quad (18)$$

The ion-molecule reactions of the $Co(CO)_3(NO)$ system illustrate the influence that the nature of the initial reactant ion has on the clustering process. In general, the M^+ and $M(CO)_x(NO)_y^+$ ions react to give different ionic cluster fragments.

$Ni(CO)_4$. Direct ionization of $Ni(CO)_4$ produces abundant ions corresponding to $Ni(CO)_x^+$ (x = 0-4). The largest cluster fragment produced by the reaction of Ni^+ with $Ni(CO)_4$ is $Ni_6(CO)_8^+$. The $Ni_6(CO)_8^+$ ion is formed by sequential reaction of $Ni_2(CO)_x^+$ (x = 2, 3), $Ni_3(CO)_{x+1}^+$, $Ni_4(CO)_7^+$, and $Ni_5(CO)_6^+$. A generalized reaction sequence is summarized in Scheme V. The reaction sequences for $Ni(CO)^+$, $Ni(CO)_2^+$, and $Ni(CO)_3^+$ are summarized in Schemes VI, VII, and VIII.

Scheme V

$$Ni^+ + Ni(CO)_4 \rightarrow Ni_2(CO)_x^+ \quad (x = 2, 3) \quad (19)$$

$$Ni_2(CO)_x^+ + Ni(CO)_4 \rightarrow Ni_3(CO)_{x+2}^+ \quad (20)$$

$$Ni_3(CO)_{x+2}^+ + Ni(CO)_4 \rightarrow Ni_4(CO)_7^+ \quad (21)$$

$$Ni_4(CO)_7^+ + Ni(CO)_4 \rightarrow Ni_5(CO)_6^+ \quad (22)$$

$$Ni_5(CO)_6^+ + Ni(CO)_4 \rightarrow Ni_6(CO)_8^+ \quad (23)$$

Scheme VI

$$Ni(CO)^+ + Ni(CO)_4 \rightarrow Ni_2(CO)_x^+ \quad (x = 3, 4) \quad (24)$$

$$Ni_2(CO)_x^+ + Ni(CO)_4 \rightarrow Ni_3(CO)_{x+3}^+ \quad (25)$$

$$Ni_3(CO)_{x+3} + Ni(CO)_4 \rightarrow Ni_4(CO)_8^+ \quad (26)$$

$$Ni_4(CO)_8^+ + Ni(CO)_4 \rightarrow Ni_5(CO)_{11}^+ \quad (27)$$

Scheme VII

$$Ni(CO)_2^+ + Ni(CO)_4 \rightarrow Ni_2(CO)_x^+ \quad (x = 3\text{-}5) \quad (28)$$

$$Ni_2(CO)_x^+ + Ni(CO)_4 \rightarrow Ni_3(CO)_{x+3}^+ \quad (29)$$

$$Ni_3(CO)_{x+3}^+ + Ni(CO)_4 \rightarrow Ni_4(CO)_9^+ \quad (30)$$

$$Ni_4(CO)_9^+ + Ni(CO)_4 \rightarrow Ni_5(CO)_{11}^+ \quad (31)$$

Scheme VIII

$$Ni(CO)_3^+ + Ni(CO)_4 \rightarrow Ni_2(CO)_x^+ \quad (x = 4\text{-}6) \qquad (32)$$

$$Ni_2(CO)_x^+ + Ni(CO)_4 \rightarrow Ni_3(CO)_y^+ \quad (y = 7, 8) \qquad (33)$$

$$Ni_3(CO)_y^+ + Ni(CO)_4 \rightarrow Ni_4(CO)_9^+ \qquad (34)$$

$$Ni_4(CO)_9^+ + Ni(CO)_4 \rightarrow Ni_5(CO)_{11}^+ \qquad (35)$$

Discussion

Electron Deficiency Model. In our first paper,[1] we proposed that the ionic cluster fragments formed in the $Cr(CO)_6$ and $Fe(CO)_5$ system can be understood by examining the electron deficiencies of the cluster fragments, as well as considering the effects of excess internal energy. In this paper we will apply these same concepts to the $Co(CO)_3(NO)$ and $Ni(CO)_4$ systems. In this way, we can test the general utility of these ideas.

By way of review, the electron deficiency (ED) of a particular ionic cluster fragment is calculated by using the 18-electron rule (eq 1)[7]

$$ED = [18n - (\text{total no. of valence electrons in the cluster})]/n \qquad (I)$$

where n equals the total number of metal atoms in the cluster. Electron deficiencies calculated by using the 18-electron rule assume that the ionic cluster fragments have the structures found in the triangular polyhedra of the boron hydrides. As an example, by using this method an electron deficiency of 0.75 is obtained for the $Ni_4(CO)_9^+$ ion (eq 2). Conversely, an electron deficiency

$$ED = [18(4) - [(4(13)) + (9(2)) - 1]]/4 = 0.75 \qquad (II)$$

of 3.5 is estimated for the $Ni_2(CO)_4^+$ ion. Since the electron deficiency is an indication of the number of open coordination sites on a metal atom, a direct correlation should exist between electron deficiency and reactivity.[2] Thus, $Ni_2(CO)_4^+$ (electron deficiency of 3.5) should have a higher relative reactivity than $Ni_4(CO)_9^+$ (electron deficiency of 0.75). On the basis of this simple concept, a plot of reactivity vs. electron deficiency should increase in a monotonic manner.[2] This concept is shown graphically in Figure 3 where we have plotted log relative reaction rate for the ionic cluster fragments formed by $Ni(CO)_3^+$ reacting with neutral $Ni(CO)_4$. Clearly, for this system a direct relationship between reactivity and electron deficiency is indicated.

However, the correlation between reactivity and electron deficiency is not always so obvious. The reactivity vs. electron deficiency data for the ionic cluster fragments formed by Ni^+ reacting with $Ni(CO)_4$ is shown in Figure 4. The simple relationship between reactivity and electron deficiency does not hold for this system. In the paper on $Cr(CO)_6$ and $Fe(CO)_5$[1] we demonstrated that the electron deficiency of a given system could be altered by the presence of multiple metal–metal bonds and/or 4- or 6-electron donating CO ligands, i.e., some ionic cluster fragments appear to have higher bond order than predicted by the 18-electron rule.

For the ionic cluster fragments formed by Ni^+ reacting with $Ni(CO)_4$ it is important to consider the coordination unsaturation of these ions. For instance, the values of the electron deficiency of $Ni_2(CO)_2^+$ and $Ni_2(CO)_3^+$ calculated by eq 1 are 5.5 and 4.5, respectively. Such high electron deficiencies should lead to high reactivities, but this is clearly not the case for $Ni_2(CO)_2^+$. The reactivity of the $Ni_2(CO)_2^+$ ion is lower by a factor of 0.9 than the reactivity of $Ni_2(CO)_3^+$. The low reactivity for the $Ni_2(CO)_2^+$ ion is consistent with the idea that this ion has a high bond order, i.e., multiple metal–metal bonds and/or CO donating four electrons. The high bond orders inferred from the reactivity/electron deficiency data can be rationalized by considering that the nickel atoms localize the metal d electrons rather than use them for ligand binding. The increase in the bond order for $Ni_2(CO)_2^+$ would result in a decrease in the electron deficiency. Therefore, a high bond order is assigned to the ionic cluster fragments which deviate from the reactivity vs. electron deficiency curve in Figure 4. That is, the ionic cluster fragments $Ni_2(CO)_2^+$, $Ni_3(CO)_4^+$, and $Ni_3(CO)_5^+$ have low reactivities; but the calculated electron deficiencies (assigning simple polyhedral structures) of these ions are high. On the other hand, if high bond orders are assigned to these ionic cluster fragments, the reactivity vs. electron deficiency curve shows a monotonic increase. Figure 5 contains the electron deficiency data for the $Ni^+/Ni(CO)_4$ system obtained by assigning high bond orders to $Ni_2(CO)_2^+$, $Ni_3(CO)_4^+$, and $Ni_3(CO)_5^+$.

On the basis of these general concepts, we propose that ionic cluster fragments which have low reactivities will have electron deficiencies which deviate from the value predicted from the

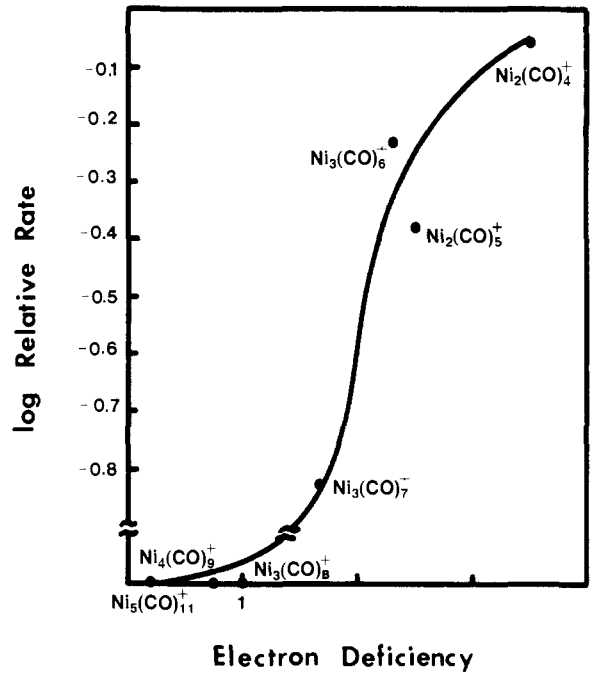

Figure 3. Plot of log relative rate vs. calculated electron deficiencies for $Ni(CO)_3^+/Ni(CO)_4$. Calculated electron deficiencies are based on simple polyhedral models of boron hydrides. The rates of the ionic cluster fragments are normalized to the rate of the $Ni(CO)_3^+$ ion.

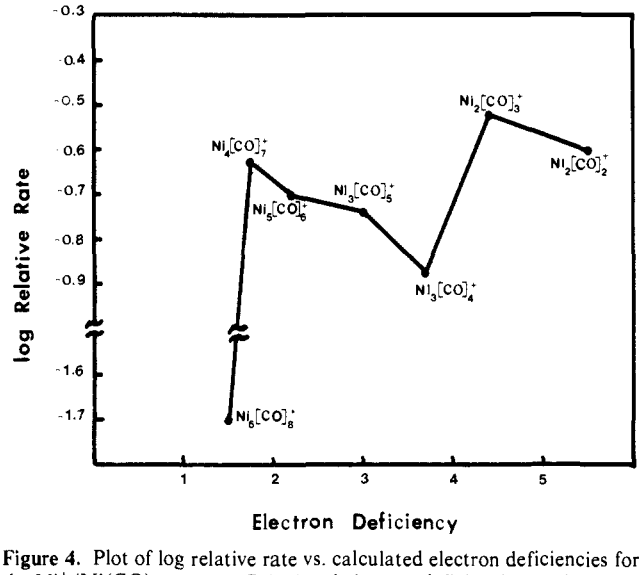

Figure 4. Plot of log relative rate vs. calculated electron deficiencies for the $Ni^+/Ni(CO)_4$ system. Calculated electron deficiencies are based on simple polyhedral models of boron hydrides. The rates of the ionic cluster fragments are normalized to the rate of the Ni^+ ion.

(6) Castro, M. E.; Russell, D. H. *Anal. Chem.* **1985**, *57*, 2290.
(7) Wade, K. "Transition Metal Cluster"; Johnson, B. F. G., Ed.; John Wiley & Sons: New York, 1980; Chapter 3.

Table I. Ionic Cluster Fragments of the $Co(CO)_3(NO)$ System

ion	log rel rate[a]	electron deficiency	ED*[b]
Reactant Ion = Co^+			
$Co_2(CO)(NO)^+$	−0.126	6.0	3.0
$Co_2(CO)_2(NO)^+$	−0.182	5.0	3.0
$Co_3(CO)_2(NO)^+$	−0.793	5.0	1.67
$Co_3(CO)_2(NO)_2^+$	0.0212	4.0	
$Co_4(CO)_2(NO)_3^+$	−0.108	3.0	
$Co_4(CO)_3(NO)_3^+$	−0.252	2.5	
$Co_5(CO)_3(NO)_4^+$	−0.383	2.0	
$Co_5(CO)_4(NO)_4^+$	−0.272	1.6	2.4
$Co_6(CO)_5(NO)_5^+$	−0.788	1.0	
$Co_6(CO)_6(CO)_5^+$	−∞[c]	0.67	
Reactant Ion = $Co(CO)^+$			
$Co_2(CO)_2(NO)^+$	0.0682	5.0	
$Co_2(CO)_3(NO)^+$	0.104	4.0	
$Co_2(CO)_4(NO)^+$	−0.180	3.0	
$Co_2(CO)_3(NO)_2^+$	−0.371	2.5	
$Co_3(CO)_2(NO)_2^+$	−0.371	4.0	3.33
$Co_4(CO)_3(NO)_3^+$	−0.481	2.5	
$Co_4(CO)_4(NO)_3^+$	−∞	2.0	1.0
$Co_5(CO)_4(NO)_4^+$	−0.742	1.6	
Reactant Ion = $Co(CO)_2^+$			
$Co_2(CO)_3(NO)^+$	−0.227	4.0	
$Co_2(CO)_2(NO)_2^+$	−0.270	3.5	
$Co_2(CO)_4(NO)^+$	−0.141	3.0	4.0
$Co_3(CO)_3(NO)_2^+$	−0.793	2.5	0.5
$Co_3(CO)_4(NO)_2^+$	−0.318	2.67	
$Co_4(CO)_4(NO)^+$	−0.807	3.5	0.25
$Co_4(CO)_5(NO)^+$	−∞	3.0	0.5
$Co_5(CO)_4(NO)^+$	−∞	3.4	1.4
Reactant Ion = $Co(CO)_2(NO)^+$			
$Co_2(CO)_3(NO)_2^+$	−∞	2.5	1.5
$Co_2(C)_4(NO)_2^+$	−0.398	3.5	
$Co_3(CO)_4(NO)_2^+$	−0.155	2.67	4.0
$Co_3(CO)_5(NO)_3^+$	−∞	1.0	1.0
$Co_4(CO)_4(NO)_3^+$	0.306	1.0	4.5

[a] The rate of the ionic cluster fragments is relative to the rate of the reactant ion. [b] The column marked ED* refers to the electron deficiency calculated assuming multiple metal–metal bonds and/or four-electron donor carbonyl ligands are present. [c] The log relative rate is defined as −∞ for those cluster fragments which have no discernable rate.

18-electron rule. Ionic cluster fragments having high bond orders will have low electron deficiencies since the number of valence electrons increases (see eq 1). That is, in cases involving multiple metal–metal bonds the number of valence electrons increases because two additional electrons are provided by each metal–metal bond.[2] Similarly, two additional valence electrons are provided by each four-electron-donating CO ligand. Thus, a CO molecule which donates four electrons and a double metal–metal bond decreases the electron deficiency by the same amount. (Exact determination of the structure of the ionic cluster fragments cannot be obtained by the present experimental technique.)

The electron deficiency data for the ionic cluster fragments also gives some indication of the Lewis acidity/basicity of the metal centers. In the ionic cluster fragments which have small electron deficiencies, the metals accept electrons from either the ligands and/or the surrounding metals. If multiple metal–metal bonds are formed this suggests that π^* back-bonding is unfavorable. Thus, the metal center of the ionic cluster fragments with low electron deficiencies can be classified as Lewis acids. Conversely, ionic cluster fragments having high electron deficiencies will have metal centers which act as Lewis bases, i.e., π^* back-bonding is favorable.

The relative reactivities and electron deficiencies for the ionic cluster fragments for each reaction sequence studied (Scheme I–IV, VI, and VII) are summarized in Tables I and II. The ionic cluster fragments for which relative reactivity and calculated electron deficiency did not correlate were assumed to have high bond order, e.g., multiple metal–metal bonds and/or carbonyl ligands acting as four-electron donors.[8] The column marked ED* gives the electron deficiency indicated by the relative reactivity data. In the case of $Co(CO)_3(NO)$, the electron deficiency calculations were made assuming NO to be a three-electron donor.

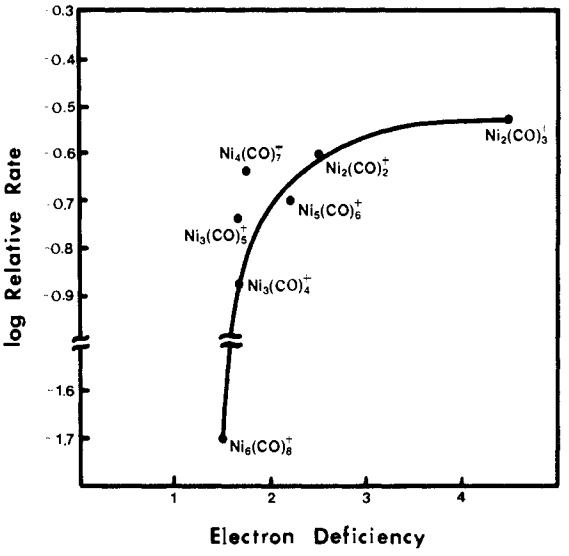

Figure 5. Plot of log relative rate vs. electron deficiency for the $Ni^+/Ni(CO)_4$ system. In this system, the electron deficiencies were calculated assuming that some of the cluster fragments contain multiple metal–metal bonds and/or carbonyl ligands acting as four-electron donors.

Table II. Ionic Cluster Fragments of the $Ni(CO)_4$ System

ion	log rel rate[a]	electron deficiency	ED*[b]
Reactant Ion = Ni^+			
$Ni_2(CO)_2^+$	−0.602	5.5	2.5
$Ni_2(CO)_3^+$	−0.523	4.5	
$Ni_3(CO)_4^+$	−0.876	3.67	1.67
$Ni_3(CO)_5^+$	−0.738	3.0	1.67
$Ni_4(CO)_7^+$	−0.633	1.75	
$Ni_5(CO)_6^+$	−0.699	2.2	
$Ni_6(CO)_8^+$	−1.69	1.5	
Reactant Ion = $Ni(CO)^+$			
$Ni_2(CO)_3^+$	−0.371	4.5	
$Ni_2(CO)_4^+$	−0.733	3.5	1.5
$Ni_3(CO)_6^+$	−0.453	2.3	
$Ni_3(CO)_7^+$	−1.35	1.67	1.0
$Ni_4(CO)_8^+$	−0.733	1.25	
$Ni_5(CO)_{11}^+$	−∞[c]	0.2	
Reactant Ion = $Ni(CO)_2^+$			
$Ni_2(CO)_3^+$	−0.207	4.5	2.5
$Ni_2(CO)_4^+$	−0.083	3.5	
$Ni_2(CO)_5^+$	−0.248	2.5	
$Ni_3(CO)_6^+$	−0.417	2.3	1.67
$Ni_3(CO)_7^+$	−0.321	1.67	
$Ni_3(CO)_8^+$	−1.13	1.0	
$Ni_4(CO)_9^+$	−∞	0.75	
$Ni_5(CO)_{11}^+$	−∞	0.20	
Reactant Ion = $Ni(CO)_3^+$			
$Ni_2(CO)_4^+$	0.0580	3.5	
$Ni_2(CO)_5^+$	−0.380	2.5	
$Ni_2(CO)_6^+$	−0.234	1.5	
$Ni_3(CO)_6^+$	−0.812	1.67	
$Ni_4(CO)_9^+$	−∞	0.75	
$Ni_5(CO)_{11}^+$	−∞	0.20	

[a] The rate of the ionic cluster fragments is relative to the rate of the reactant ion. [b] The column marked ED* refers to the electron deficiency calculated assuming multiple metal–metal bonds and/or four-electron donor carbonyl ligands are present. [c] The log relative rate is defined as −∞ for those cluster fragments which have no discernable rate.

(8) The positive charge on the ionic cluster fragments was considered to be part of the valence electrons and was included in the calculation of the electron deficiencies.

In some cases (e.g., $Co_5(CO)_4(NO)_4^+$ in Scheme I, $Co_2(CO)_4(NO)^+$ in Scheme II, and $Co_3(CO)_4(NO)_2^+$ and $Co_4(CO)_4(NO)_3^+$ in Scheme IV) it appears that the NO ligand is a 1-electron donor.

Cluster Valence Molecular Orbital Model. The concept of electron deficiencies and bond order of the ionic cluster fragments share many similarities with the cluster valence molecular orbital model developed by Lauher.[3] Lauher describes the molecular orbitals of transition-metal clusters to be of two types: high-lying antibonding orbitals (HLAO) and cluster valence molecular orbitals (CVMO). According to Lauher, the HLAO are too high in energy to accept electrons from ligands or contain nonbonding electrons. The CVMO, on the other hand, are accessible to either ligand or metal electrons. The stoichiometry of a cluster is determined by its geometry and not by the identity of the metals or the ligands.[9] Therefore, a cluster with a particular size or geometry has a certain number of bonding CVMO. For example, a tetrahedron has 30 CVMO available for cluster bonding while a trigonal bipyramid will have 36 CVMO. The number of cluster valence electrons (CVE) for a tetrahedron would then be 60 (2 electrons for every CVMO). In the CVMO model electron deficiency or unsaturation corresponds to a decrease in the number of CVE. Lauher suggests that "Unsaturated (or electron deficient) clusters can be expected to show unusual reactivity. Such a cluster would in general readily react with additional ligands to achieve the proper number of CVE."[3]

On the basis of the electron deficiency model, the reactivity of a particular ionic cluster fragment is due to the electron deficiency. This concept is consistent with the basic ideas of Lauher's CVMO model, e.g., the reactivity of a cluster or ionic cluster fragment is determined by the number of unoccupied CVMO. For example, a tetrahedron has 30 CVMO (60 CVE), but if the cluster has one unoccupied CVMO (i.e., 58 CVE) the cluster would tend to add an additional 2-electron-donating ligand. Similarly, an electron deficient ionic cluster fragment would react with additional ligands to satisfy this deficiency.

The sequence of reactions leading to formation of the ionic cluster fragments can be generalized as follows. The ionic cluster fragments formed by ion–molecule reactions which follow the simple polyhedral model react with the neutral to add 14 electrons. The addition of 14 electrons is favored because this gives the proper number of ICVE. A general reaction scheme is given below (Scheme IX).

Scheme IX

$$M^+ + 14e^- \rightarrow M_2^+ \quad (36)$$

$$M_2^+ + 14e^- \rightarrow M_3^+ \quad (37)$$

$$M_3^+ + 14e^- \rightarrow M_4^+ \text{ etc.} \quad (38)$$

The addition of 14 electrons to an ionic cluster fragment corresponds to the addition of a ligand to achieve the proper number of CVE. An excellent example of 14-electron addition is found in the Cr^+ reaction scheme.[1] $Cr_2(CO)_4^+$ (19 ICVE) reacts with $Cr(CO)_6$ (by addition of $Cr(CO)_4$) to give $Cr_3(CO)_8^+$ (33 ICVE). The addition of $Cr(CO)_4$ to $Cr_2(CO)_4^+$ initially corresponds to addition of a ligand ($Cr(CO)_4$) to form $[Cr_2(CO)_4...L]^+$ where L = $Cr(CO)_4$. The $[Cr_2(CO)_4...L]^+$ species has the proper number of ICVE (33) needed for a dimer. However, once the proper number of ICVE is obtained, $[Cr_2(CO)_4...L]^+$ rearranges to a stable trimer, i.e., $Cr_3(CO)_8^+$. $Cr_3(CO)_8^+$ has 33 ICVE and is very unsaturated. Therefore, $Cr_3(CO)_8^+$ reacts with $Cr(CO)_6$, again adding 14 electrons ($Cr(CO)_4$). The resulting species $[Cr_3(CO)_8...L]^+$ rearranges to a stable tetrahedron, $Cr_4(CO)_{12}^+$. According to the CVMO formulism, $Cr_2(CO)_4^+$ and $Cr_3(CO)_8^+$ are "reacting with additional ligands (e.g., $Cr(CO)_4$) to achieve the proper number of CVE".

Similar reactions corresponding to the addition of 14 electrons are observed for the Fe, Co, and Ni systems. However, in these systems the number of ICVE in the product ionic cluster fragments is higher than predicted. For example, the addition of 14 electrons of $Fe_2(CO)_4^+$ gives rise to 37 ICVE instead of 34 expected for a dimer. This higher number of ICVE can be accommodated since the ionic cluster fragments will undergo rearrangement. That is, the Fe, Co, and Ni ionic cluster fragments add 14 electrons to obtain the proper number of ICVE. However, once the proper number of ICVE is obtained, the ionic cluster fragment will undergo rearrangement analogous to that found for Cr, e.g., a dimer rearranges to a trimer. This rearrangement is due to the inclusion of a metal atom in the 14 ligand electrons that are being added. $Cr_x(CO)_y^+$ ionic cluster fragments are formed by addition of $Cr(CO)_4$ (6 electrons from Cr and 8 electrons from $(CO)_4$), whereas $Fe_x(CO)_y^+$ ionic cluster fragments are formed by the addition of $Fe(CO)_3$ (8 electrons from Fe and 6 electrons from $(CO)_3$). Once the proper number of ICVE has been achieved, the d electrons of $Fe(CO)_3$ interact with the d block CVMO of $Fe_2(CO)_4^+$, giving rise to a different metal core cluster and creating new CVMO. Similarly, $Co_x(CO)_y(NO)_z^+$ ionic cluster fragments are formed by the addition of Co(CO)(NO) (9 electrons from Co, 2 electrons from CO, and 3 electrons from NO), and $Ni_x(CO)_y^+$ ionic cluster fragments are formed by the addition of $Ni(CO)_2$ (10 electrons from Ni and 4 electrons from $(CO)_2$).

The creation of new CVMO also explains why the ionic cluster fragments continue to react once 14 electrons are added. Owing to a deficiency in the number of ICVE, $Fe_2(CO)_4^+$ reacts with $Fe(CO)_5$ to add $Fe(CO)_3$ and the resulting ionic cluster fragment, $Fe_3(CO)_7^+$, does not have the proper number of ICVE (ICVE = 37) for a trimer (CVE = 48). Thus, $Fe_3(CO)_7^+$ reacts with $Fe(CO)_5$ again to add 14 electrons and forms $Fe_4(CO)_{10}^+$. This sequence (Scheme IV in our previous paper[1]) continues and terminates with the production of $Fe_6(CO)_{18}^+$. $Fe_6(CO)_{18}^+$ has 83 ICVE which is the proper number for a bicapped tetrahedron. The $Fe_6(CO)_{18}^+$ ionic cluster fragment is electronically saturated and does not react further.

The reaction sequence for $Ni(CO)_3^+$ (Scheme VIII) proceeds in a similar manner. Each reactant ionic cluster fragment adds 14 electrons ($Ni(CO)_2$), achieves the proper number of ICVE, creates new CVMO, and continues to react. $Ni_5(CO)_{11}^+$, the terminal ion in this reaction sequence, has 71 ICVE which is the number of CVE found in a trigonal bipyramid. Owing to the fact that $Ni_5(CO)_{11}^+$ is electronically saturated it does not react further.

The question that now arises is why do some ionic cluster fragments react to add a ligand containing fewer than 14 electrons? That is, why are some ionic cluster fragments being formed which have high bond orders? For example, $Fe_2(CO)_4^+$ reacts with $Fe(CO)_5$ to form $Fe_3(CO)_6^+$, i.e., addition of $Fe(CO)_2$ (12 electrons). While it appears that $Fe_2(CO)_4^+$ has reacted to add 12 electrons, the actual number of added electrons may be higher if the CO molecules donate four electrons. That is, the addition of $Fe(CO)_2$, where one CO molecule acts as a 4-electron donor, corresponds to the addition of 14 electrons.

The increase in bond order for some ionic cluster fragments, and therefore the variation in the number of electrons added, is also consistent with the CVMO theory. Lauher states that unsaturated clusters may be unusually reactive or "the metal core of the [unsaturated] clusters might isomerize to a different geometry with the proper number of CVMO or one of the existing ligands might bind in an unusual manner such that more of its electrons are formally donated to the metal".[3] Lauher uses $Os_3H_2(CO)_{10}$ and $Fe_4(CO)_{13}H^-$ as examples of this type of chemistry. The metal core of $Os_3H_2(CO)_{10}$ has two normal Os–Os bond lengths and one short Os–Os bond distance (a double bond) and deviates considerably from the D_{3h} geometry assigned to trimers. $Fe_4(CO)_{13}H^-$ appears to have 60 CVE which is the correct number for a tetrahedron. However, one of the CO ligands of this cluster donates four electrons[10] resulting in 62 CVE and the C_{2v} butterfly geometry. Similar rearrangement reactions are suggested for the ionic cluster fragments with high bond orders. Thus, the variation in the number of electrons added to the ionic

(9) Lauher, Joseph W. *J. Am. Chem. Soc.* **1979**, *101*, 2604.

(10) Manassero, M.; Sansoni, M.; Longoni, G. *J. Chem. Soc., Chem. Commun.* **1976**, 919.

cluster fragment upon reaction with the neutral metal carbonyl is the result of either the CO ligands binding in an unusual manner or isomerization of the core metal cluster to a different structure. For the former case, the number of ICVE present will be greater than the number suggested by the molecular formula. In the latter case, isomerization to a different geometry changes the number of CVMO available, causing a change in the ICVE.

In the Results section, particular emphasis was made regarding the differences in the cluster formation patterns for Co^+ (Scheme I) and $Co(CO)_2^+$ (Scheme III). These differences can now be explained in terms of the CVMO model. Co^+ reacts with $Co(CO)_3(NO)$ to form $Co_2(CO)(NO)^+$, $Co_3(CO)_2(NO)_2^+$, $Co_4(CO)_3(NO)_3^+$, $Co_5(CO)_4(NO)_4^+$, and $Co_6(CO)_5(NO)_5^+$, e.g., addition of Co(CO)(NO) (14 electrons) to the reactant ion. These ionic cluster fragments have bond orders which are consistent with polyhedral structures. The ionic cluster fragments formed by the reaction of $Co(CO)_2^+$ are quite different from those formed by reaction of Co^+, e.g., $Co_3(CO)_4(NO)_2^+$ reacts with $Co(CO)_3(NO)$ to form $Co_4(CO)_x(NO)^+$ (x = 4, 5). $Co_3(CO)_4(NO)_2^+$ has 36 ICVE (the NO is a one-electron donor). When $Co_3(CO)_4(NO)_2^+$ reacts with $Co(CO)_3(NO)$ to form $Co_4(CO)_x(NO)_+$, the product ion isomerizes to a different geometry than expected for a tetramer. A four metal atom cluster can have one of four geometries, a T_d, C_{3v}, D_{2h}, and D_{4h} geometry. The T_d geometry has the smallest number of CVMO (30) while the D_{4h} geometry has the largest number of CVMO (32). The reactivity for $Co_4(CO)_4(NO)^+$ is very low, indicating that this ionic cluster fragment has a high bond order. According to the electron deficiency model, $Co_4(CO)_4(NO)^+$ has a tetrahedral structure with either four double metal–metal bonds and three CO ligands which are four-electron donors or three double metal–metal bonds and four CO ligands which are four-electron donors. The presence of multiple metal–metal bonds in $Co_4(CO)_4(NO)^+$ decreases the number of CVMO and therefore the number of ICVE. As a result, $Co_3(CO)_4(NO)_2^+$ will react with $Co(CO)_3(NO)$ to add fewer than 14 electrons.

For the electron deficiency vs. relative reaction rate analogy, we chose to use the 18-electron model to calculate the electron deficiencies because of the low nuclearity of the ionic cluster fragments. There are cases, i.e., the large ionic cluster fragments such as $Co_6(CO)_6(NO)_5^+$, where use of the CVMO counting system would create a large difference in the electron deficiency found with the 18-electron model. However, this difference is not important since the large ionic cluster fragments (which have a low electron deficiency even when the 18-electron model is used) have a low relative reaction rate. We then begin to see a parallel between the electron deficiency model and CVMO model. For both models, the number of electrons present in the ionic cluster fragment is determined by the structure (geometry) of the ionic cluster fragments. Both models also explain the differences in reactivity of the ionic cluster fragments. Although both the electron deficiency model and CVMO model can explain the data for the clustering sequence in the Cr, Fe, Co, and Ni systems, the CVMO model offers a higher level of understanding.

Stability of Ionic Cluster Fragments. A detailed inspection of reaction Schemes I–VIII reveals many similarities but some important differences. Of particular interest is the difference in reactivity of the ionic cluster fragments formed by $Co(CO)^+$ and $Co(NO)^+$. $Co(CO)^+$ reacts with $Co(CO)_3(NO)$ to form several dinuclear species, the most reactive being $Co_2(CO)_3(NO)^+$. The dinuclear ionic cluster fragments react further with neutral $Co(CO)_3(NO)$ to form $Co_3(CO)_2(NO)_2^+$ (Scheme II). Conversely, $Co(NO)^+$, reacts to form $Co_2(CO)_3(NO)_2^+$ which does not react further. The difference between the dinuclear species $Co_2(CO)_x(NO)^+$ (x = 2–4) and $Co_2(CO)_3(NO)_2^+$ could be related to the ability of NO to stabilize the product ion. The π^* orbital of NO is at least 3.7 eV more stable than the π^* orbital of CO.[11] Therefore, NO is more effective than the CO in terms of π stabilization. As a result of the π stabilization, the reaction coordinates for $Co(CO)^+$ and $Co(NO)^+$ differ significantly and this effect will influence both the reactivity of the ionic cluster fragments as well as the ionic cluster fragments formed by subsequent reactions.

Further evidence which suggest strong ligand effects on the reactivity can be found in the $Cr(CO)_6$ system. In some respects, the chemistry of Cr^+ and $Cr(CO)^+$ are similar to the chemistry of the $Co_2(CO)_x(NO)^+$ (x = 2–4) and $Co_2(CO)_3(NO)_2^+$ ions formed by $Co(CO)^+$ and $Co(NO)^+$. Although carbon monoxide is not as effective at π stabilization as NO, CO will have a stabilizing effect on the bare metal ion. Therefore, due to the π stabilization of CO, the reaction coordinates for Cr^+ and $Cr(CO)^+$ differ and give rise to product ions having different reactivities. Note that the relative reactivity of $Co_2(CO)_3(NO)_2^+$ is dependent upon whether it is formed by $Co(NO)^+$ or $Co(CO)(NO)^+$ (Table I). These data also suggest that ligand effects play an important role in the ion–molecule chemistry of ionic cluster fragments. In studies on the reactivity of Co_2^+ and $Co_2(CO)^+$, Ridge has noted similar ligand effects. That is, Co_2^+ is unreactive, i.e., does not undergo C–C and C–H bond insertions, whereas $Co_2(CO)^+$ readily undergoes C–H bond insertion reactions with simple alkanes.[12]

A basic premise of the electron deficiency model is that ionic cluster fragments with low electron deficiencies are intrinsically more stable than cluster fragments with high electron deficiencies. Tables I and II show that some cluster fragments with low electron deficiencies and reactivities lose a ligand(s) to produce other ionic cluster fragments with higher electron deficiencies (presumably less stable). For example, the $Co_4(CO)_3(NO)_3^+$ ion formed by reaction of Co^+ with $Co(CO)_3(NO)$ has an electron deficiency of 2.5. This ion expels CO to give $Co_4(CO)_2(NO)_3^+$ which has an electron deficiency of 3.0. Owing to the exothermicity of the ion–molecule reaction, the $Co_4(CO)_3(NO)_3^+$ ion is probably formed with excess internal energy and without collisional stabilization decays by unimolecular expulsion of the CO ligand. Loss of this ligand results in a cluster that has a higher electron deficiency (3.0) and is therefore more reactive. A similar trend was noted and discussed for the $Cr(CO)_6$ and $Fe(CO)_5$ system. Thus, while the reactivity of an ionic cluster fragment is dependent upon the electron deficiency, the ionic cluster fragments formed by a given system, e.g., $M_j(CO)_m(NO)_n^+/M(CO)_x(NO)_y$, will depend on the relative stability of the cluster fragment and the energetics of the ion–molecule reaction.

Conclusions

In this paper we have attempted to expand the ideas and concepts developed for the $Cr(CO)_6$ and $Fe(CO)_5$ systems to the ionic cluster fragments formed in the $Co(CO)_3(NO)$ and $Ni(CO)_4$ systems. The degree of coordination unsaturation of the ionic cluster fragments formed by $Co(CO)_3(NO)$ and $Ni(CO)_4$ is explained by comparing the electron deficiency and relative reaction rates of the ionic cluster fragments.[1,2] On the basis of this analogy, we propose the existence of ionic cluster fragments in the $Co(CO)_3(NO)$ and $Ni(CO)_4$ systems which have a high bond order and/or four-electron-donor CO's.

Comparison of the $Cr(CO)_6$, $Fe(CO)_5$, $Co(CO)_3(NO)$, and $Ni(CO)_4$ systems shows that the ionic cluster fragments with simple polyhedral structures are formed by the sequential addition of 14 electrons. The addition of 14 electrons follows the bonding concepts in transition-metal clusters proposed by Lauher. The number of CVE in a polyhedron is approximately equal to the ICVE found in the ionic cluster fragments. The ionic cluster fragments which have a high bond order have multiple metal–metal bonds and/or four-electron-donating CO's so that they, too, can have ICVE which approach the number of CVE found in transition-metal clusters.

One difference that stands out in the ion–molecule reaction chemistry of $Cr(CO)_6$, $Fe(CO)_5$, $Co(CO)_3(NO)$, and $Ni(CO)_4$ is the degree of coordination unsaturation of the ionic cluster fragments. Ionic cluster fragments formed by Cr are, on the average, more unsaturated than the cluster fragments formed by Co, Fe, and Ni. We feel that this difference in unsaturation is

(11) Lloyd, D. R.; Schlag, E. W. *Inorg. Chem.* **1969**, *8*, 2544.

(12) Freas, R. B.; Ridge, D. P. *J. Am. Chem. Soc.* **1984**, *106*, 825.

a periodic effect and is due to the fact that Cr is a group 6 metal while Co, Fe, and Ni are group 8 metals.

This study provides a guide based on bond order, structure, and reactivity for additional studies on the ion-molecule chemistry of the ionic cluster fragments. Currently, we are examining the ion-molecule chemistry of heteroatom ionic cluster fragments (e.g., Co/Ni, Cr/Ni, Fe/Ni, Cr/Fe, Co/Fe, and Co/Cr) to probe further the relationship between the CVMO theory and the reaction sequence of the ionic cluster fragments.

In addition, more detailed studies on ligand effects are underway. In these studies we are comparing the cluster formation sequences of ions such as MH^+, MCO^+, and MNO^+. Studies with these and additional ligand systems are designed to investigate ligand effects on the nature of the ionic cluster fragments formed and the influence of the initial ligand on the degree of coordination unsaturation of the ionic cluster fragment product ions.

Acknowledgment. This work was supported by the U.S. Department of Energy, Office of Basic Energy Sciences (DE-A505-82ER13023). Some of the TAMU Equipment was purchased from funds provided by the TAMU Center for Energy and Mineral Resources. We gratefully acknowledge the Texas Agriculture Experimental Station which provided a fraction of the funds for purchase of the Nicolet FTMS 1000 spectrometer.

Binding of Alkenes to the Ligands in OsO_2X_2 (X = O and NR) and $CpCo(NO)_2$. A Frontier Orbital Study of the Formation of Intermediates in the Transition-Metal-Catalyzed Synthesis of Diols, Amino Alcohols, and Diamines

Karl Anker Jørgensen and Roald Hoffmann*

Contribution from the Department of Chemistry, Baker Laboratory, Cornell University, Ithaca, New York 14853. *Received July 31, 1985*

Abstract: The concerted [3 + 2] cycloaddition of an alkene to the oxygen ligands in osmium tetroxide and the binding of the alkene to the metal center leading to an asymmetric intermediate are analyzed from the frontier orbital point of view. It is suggested that the increased reactivity of osmium tetroxide with alkenes in the presence of tertiary amines, e.g., pyridine, follows from a cis addition of pyridine to osmium tetroxide, leading to a geometrical distortion of the osmium tetroxide fragment from T_d to an activated C_{2v} symmetry. The calculations are supported by the structure of the products. The reactions of d^0 bis(imido)oxoosmium species with alkenes are examined in a similar way. The reactions of a seemingly very different, yet in fact similar (η^5-cyclopentadienyl)dinitrosocobalt complex have also been analyzed from a frontier orbital point of view. The valence MO's are constructed from the cobalt dinitrosyl cation and cyclopentadienyl anion. The structure of the nitrosyl groups (bent or linear) is studied, and it has been found that the bent structure has the lowest energy. The binding of alkenes to the nitrosyl ligands is examined.

The reaction of alkenes with osmium tetroxide to form *cis*-diols is an old and well-established reaction.[1] The reaction takes place via an osmium(VI) intermediate, **1**, which on reductive or oxidative hydrolysis yields the corresponding *cis*-diol. The osmium(VI)

1

intermediate is usually written as a tetrahedral species, **I**.[2] Although it may exist as a transient complex in solution, tetrahedral **1** would be unlikely to be stable in the solid state, as it is a tetrahedral d^2 complex; there are few examples of tetrahedral d^2 stereochemistry for third-row transition metals.[3] In nonreducing solvents, alkenes (R) react with osmium tetroxide to give products of stoichiometry $OsO_4{\cdot}R$ and $OsO_5{\cdot}R_2$.[4] These products have recently been found to be dimeric monoester complexes, *syn*- and *anti*-$[Os_2O_4(O_4R)_2]$ (**2** and **3**), and monomeric diester complexes, $[OsO(O_2R)_2]$ (**4**).[5]

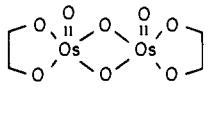

2

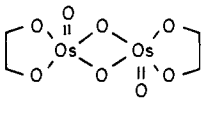

3

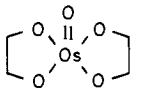

4

The initial addition of osmium tetroxide is accelerated by tertiary bases, especially pyridine.[6] The molecular structures of

(1) (a) Makowka, O. *Chem. Ber.* **1908**, *41*, 943. (b) See e.g.: March, J. "Advanced Organic Chemistry"; McGraw-Hill: New York, 1977; p 748. And: Fieser, L. F.; Fieser, M. "Reagents for Organic Synthesis"; Wiley, New York, 1985; Vol. 1-6.

(2) (a) Cotton, F. A.; Wilkinson, G. "Advanced Inorganic Chemistry", 3rd. ed.; Interscience: New York, 1972; p 1003. (b) House, H. O. "Modern Synthetic Reactions", 2nd ed.; Benjamin: San Francisco, CA, 1972; p 277.

(3) (a) Schroder, M. *Chem. Rev.* **1980**, *80*, 187. (b) The Sharpless group has recently characterized such an adduct from $Os(NR)_4$ and dimethyl fumarate, private communication.

(4) (a) Criegee, R. *Ann.* **1936**, *522*, 75; *Angew. Chem.* **1937**, *50*, 153; **1938**, *51*, 519.

(5) (a) Marzilli, L. G.; Hanson, B. E.; Kistenmacher, T. J.; Epps, L. A.; Steward, R. C. *Inorg. Chem.* **1976**, *15*, 1661. (b) Collin, R. J.; Jones, J.; Griffith, W. P. *J. Chem. Soc., Dalton Trans.* **1974**, 1094. (c) Phillips, F. L.; Skapski, A. C. *Ibid.* **1975**, 2586. (d) Phillips, F. L.; Skapski, A. C. *Acta Crystallogr., Sect. B* **1975**, *31*, 1814. (e) Collins, R. J.; Griffith, W. P.; Phillips, F. L.; Skapski, A. C. *Biochem. Biophys. Acta* **1973**, *320*, 745. (f) Collins, R. J.; Griffith, W. P.; Phillips, F. L.; Skapski, A. C. *Ibid.* **1974**, *354*, 152.

0002-7863/86/1508-1867$01.50/0